Available online at www.sciencedirect.com
SCIENCE DIRECT®
ELSEVIER
Nuclear Instruments and Methods in Physics Research B 209 (2003) 26–31
NIM B
Beam Interactions with Materials & Atoms
www.elsevier.com/locate/nimb

Spectroscopy of Si-Auger electrons from the center of heavy-ion tracks

G. Schiwietz [a,*], M. Roth [a], K. Czerski [a], F. Staufenbiel [a], M. Rösler [a], P.L. Grande [b]

[a] *Hahn-Meitner-Institut, Bereich Festkörperphysik, Glienicker Str. 100, 14109 Berlin, Germany*
[b] *Instituto de Física, Universidade Federal do Rio Grande do Sul, 91500 Porto Alegre, Brazil*

Abstract

High resolution electron spectra haven been taken for fast heavy ions at 1.78 and 5 MeV/u as well as for electrons of equal velocity incident on atomically clean Si targets. Various LVV-Auger electron structures are identified and for amorphous Si these peaks show a shift towards lower energy when the charge of the projectile is increased. This finding points to a nuclear-track potential inside the ion track. The comparison of the Auger electron spectra for amorphous Si and crystalline Si(1 1 1) 7×7 gives clear evidence for phase effects in the short-time dynamics of ion tracks.
© 2003 Elsevier B.V. All rights reserved.

PACS: 79.20.Rf; 79.20.Fv; 72.20.Jv; 32.80.Hd; 31.70.Hq; 72.15.Lh
Keywords: Nuclear-track potential; Phase effects; Multiple ionization; Auger electron-spectra; Si(1 1 1)

1. Introduction

One of the most important problems in the fields of ion-solid and laser-solid interactions is to gain knowledge about charge neutralization and electronic relaxation mechanisms in the case of dense electronic excitations. Charged regions [1,2] as well as hot electrons [3–5] on a nanoscopic scale trigger the subsequent atomic motion and rearrangement inside ion tracks [2,6]. The corresponding scenarios are *Coulomb explosion* [1] due to the mutual repulsion of ionized target atoms, spontaneous lattice relaxation due to *long lived repulsive states* [3] and the thermal spike due to *electron-phonon coupling* [4] or individual *electron-ion collisions* [5]. These mechanisms may finally yield an unordered atomic motion and if a critical local lattice temperature is exceeded, permanent atomic rearrangement may result on a time scale of 0.1–10 ps.

In previous investigations, it was possible to distinguish between the appearance of a nuclear-track potential in some polymers [7–10], related to Coulomb explosion, and high electron temperatures in the semi-metal graphite as well as in graphite-like amorphous carbon [10–12]. The nuclear-track potential, resulting from ionization and charge separation in the ion track, leads to decelerated convoy electrons [9,10] and Auger electrons

* Corresponding author. Tel.: +49-30-8062-24-48; fax: +49-30-8062-22-93.
E-mail address: schiwietz@hmi.de (G. Schiwietz).

0168-583X/$ - see front matter © 2003 Elsevier B.V. All rights reserved.
doi:10.1016/S0168-583X(02)01995-X

[7,8,10]. The corresponding positive potential attracts electrons and repels the fastest positively charged light target ions [13].

In this work, we focus on the investigation of intensities and line positions of Si target Auger-electrons. For the first time, amorphous and crystalline semi-conductor phases are compared in such an investigation of the short-time evolution of ion tracks. After a brief explanation of the experimental methods, an analysis of the data as well as electron and ion-induced Si-Auger spectra are presented.

2. Experimental method

The experiments have been performed with fast highly charged particles at velocities of 6–10% the speed of light (at 1.78 and 5 MeV/u) delivered by the heavy-ion cyclotron of the Ionenstrahl-Labor (ISL) at the Hahn-Meitner-Institut, Berlin. The setup is described in detail in [14] and thus only a brief explanation shall be given here. The heavy-ion beam of 100–500 nA was focussed to a spot size of 2×2 mm at the target (normal incidence) inside a magnetically shielded scattering chamber. A stripper foil directly in front of this chamber allows to choose a quasi-equilibrium charge-state distribution. This method was applied for 5 MeV/u Ne^{9+} and Ar^{16+} as well as 1.78 MeV/u Xe^{31+} ions. We also present data for the non-equilibrium charge-state ions 1.78 MeV/u Xe^{15+}. In this case, we estimate that about 1.5 projectile electrons will be stripped off within the first three surface layers (corresponding to the mean free path for the investigated Auger lines), leading to a slightly enhanced mean projectile charge-state.

Electron spectra haven been taken for heavy ions as well as for electrons of equal velocity (1 and 2.7 keV at an incidence angle of 45°). During the experiments, the electron beam ($\varnothing < 1$ mm) is focussed at the centre of the ion irradiated spot with an uncertainty of about ± 0.5 mm. As has been shown in a previous work for carbon targets [15], Auger electrons ejected in backward directions are mainly induced directly by the projectile (in the central track region). Thus, electron spectra with an energy resolution of about 1.7% were taken for a detection angle of 135° with respect to the ion-beam direction, corresponding to 45° with respect to the surface normal.

The surfaces of the boron doped ($<1\ \Omega$ cm) Si (1 1 1) samples are initially etched chemically and sputter cleaned. All experiments have been performed under UHV conditions (about 10^{-10} mbar, dominated by H_2). The atomically clean target surfaces (all-over contaminations <3 at.%) were characterized by Auger-electron spectroscopy and low-energy electron diffraction (LEED) before and after the ion-irradiation cycles that were lasting a few hours, dependent on the actual vacuum conditions. In between, sputtering with 5 keV Ar ions for about 20 min was used to clean the samples. Target heating up to 850 °C was performed for about 20 min to recrystallize the sample and to produce the 7×7 reconstructed surface. Afterwards the surface crystal-structure was analyzed using LEED. A LEED picture for the 7×7 surface reconstruction of Si (1 1 1), taken directly at the end of a swift heavy ion irradiation, is displayed in Fig. 1. It shows the fringes of the central spot (0 0) as well as six first-order diffractions spots (the corners of the honeycomb structure) connected by six superstructure spots. In the

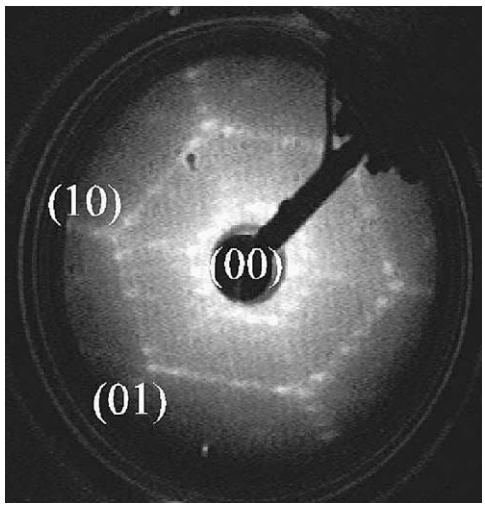

Fig. 1. Rear-view LEED pattern of Si(1 1 1) 7×7. Reciprocal surface-lattice directions, e.g. (10) are indicated. The electron gun, operated at 64 eV, is visible as dark central area with its holder pointing to the upper right corner.

following, we mainly present results for amorphized Si samples, irradiated for a few minutes with 5 keV Ar^+ ions. The amorphous structure was verified by the absence of any LEED spots before and after the measurement cycles. To avoid recrystallization due to the heat load by the fast heavy-ion beam, a special sample holder with improved cooling rates was used for the experiments with amorphized samples. Ion and electron-induced electron spectra obtained with these well-characterized Si surfaces are analyzed and presented in the next sections.

3. Auger line-intensities

The ion-induced target Auger spectrum of Si involves Auger structures at energies between 88 and 132 eV due to one up to four L-shell vacancies in the 2p shell ($2p^1VV$, $2p^2VV$, $2p^3VV$ and $2p^4VV$). Furthermore, a vacancy in the 2s shell leads to fast $2s2p^mV$ Koster–Kronig transitions (intrashell Auger decay) at energies up to 40 eV, where one 2p electron (out of 6-m) fills the 2s-hole by transferring energy to a valence electron. In the following, line intensities will be used to derive information on the initial degree of ionization inside the track. Fig. 2 displays integrated Auger yields Y_n (for $n = 2, \ldots, 4$ and Y_{2s2pV}), normalized to the sum of all $2p^iVV$ intensities (with $i = 1, \ldots, 4$), as function of the electronic perturbation parameter or interaction strength $P = |q_{\text{eff}}|/v_p$, as it appears in quantum mechanical matrix elements for electronic excitations. The projectile velocity in units of the Bohr velocity (2.19×10^6 m/s) is denoted v_p, and the effective charge q_{eff} is set equal to the mean particle charge state for most projectiles. Only for the non-equilibrium ions 1.78 MeV/u Xe^{15+} ($q_{\text{eff}} = 21$) and for 0.94 MeV/u S^{6+} ($q_{\text{eff}} = 9$, displayed in Fig. 3), we have modified q_{eff} considering projectile electron-loss and reduced screening. The experimental data points shown in Fig. 2 have been obtained as described in [14] but with an

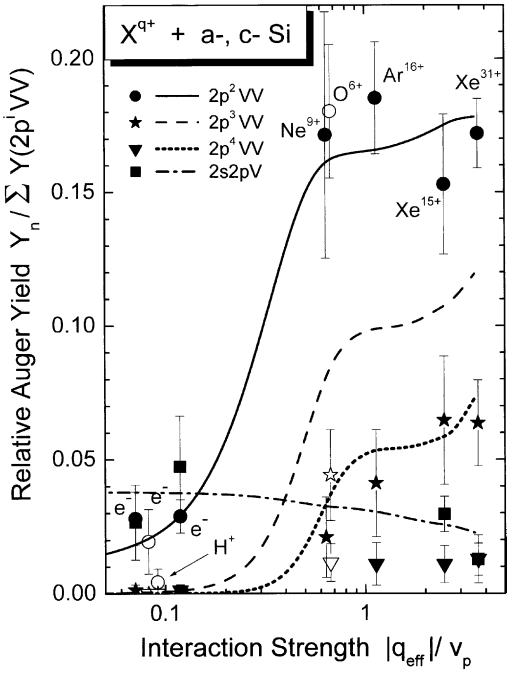

Fig. 2. Normalized experimental (symbols) and theoretical (lines) Auger yields as function of the electronic interaction strength. The open symbols have been extracted from the spectra by Schmidt et al. [16] for electrons, H^+ and O^{6+}. The main Auger intensity Y(2pVV) is equal to $1 - \sum_{n=2}^{4} Y(2p^nVV)$.

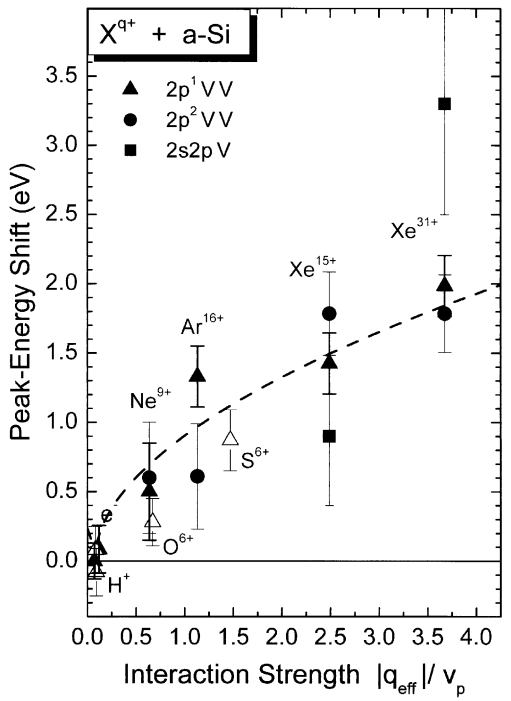

Fig. 3. Auger energy reduction versus $P = |q_{\text{eff}}|/v_p$. The open symbols have been extracted from the spectra by Schmidt et al. [16] for electrons, H^+, O^{6+} and S^{6+}.

improved accuracy of the background fits. Furthermore, we have included theoretical results and we have reanalyzed the spectra from the pioneering work by Schmidt et al. [16]. It is noted that the results by Koyama et al. [17] have been excluded, since electron reference-spectra are missing. The error bars in Fig. 2 indicate all-over estimates of the uncertainty.

The theoretical treatment is based on the Magnus approximation [10,18] (including shake-off) for ionization of the 2s0, 2p0, and 2p ± 1 states given by the Si Hartree–Fock–Slater potential. The resulting unitarized ionization probabilities for 5 MeV/u have been converted into multiple-ionization cross sections using the (statistical) independent electron model (IEM). Auger cascades have also been considered as explained below. The 2pVV Auger transition corresponds to a decay time of 45 fs, whereas the 2s2pV Koster–Kronig decay time is only 0.6 fs [19]. Using simple statistics we estimate that the Koster–Kronig decay is faster than the $2p^nVV$ Auger transitions, even for a 4-fold ionized 2p shell ($n = 4$). Thus, 2s vacancies will lead to a 2s2pV transition, increasing the number of 2p holes from n to $n + 1$. Afterwards, the $2p^nVV$ transitions will take place, leading to a remaining $(n - 1)$-fold ionized 2p shell. In this way, a whole series of Auger electrons results from one multiple-ionization event. At this point the theoretical results would represent a quasi-atomic case.

Thus, corrections for the electron escape-depth and for δ-electron cascades inside the solid have been applied. Fast δ-electrons may produce single L-shell vacancies far away from the track. As we have estimated from our previous work for C targets [8,15], considering the differences in back-scattering yields and binding energies between C and Si, the total Auger-electron yield in Si contains a 30% fraction due to these δ-electron cascades and subsequent $2p^1VV$ transitions. Furthermore, transport calculations of the energy dependent electron escape-depths were performed including penetration of the surface barrier [20] with a focus on the high-energy behavior of the electron energy-loss spectrum for homogeneously distributed electron sources at the experimental line positions. The emitted electron intensities have been integrated in the same way as for the experimental data. The resulting emission weight-factors are 0.50 (2s2pV), 1 ($2p^1VV$), 1.24 ($2p^2VV$), 1.57 ($2p^3VV$) and 1.93 ($2p^4VV$) for the different Auger lines. The final yield curves for $2p^nVV$ are proportional to P^{2n-2} for small values of the perturbation parameter P (perturbation limit of the IEM) and for large values of P they nearly reach a plateau. Exceptions are the curves for $2p^2VV$ transitions, where an offset due to shake-off processes is included, and for 2s2pV transitions which result also from single ionization in the case of small P.

Comparison of the experimental and theoretical results for $2p^1VV$ (not shown in the figure) and $2p^2VV$ shows reasonable agreement. However, discrepancies become significant for the less intense lines and reach a factor of 5 for the $2p^4VV$ decay which involves the highest observed degree of multiple ionization. This reflects a well-known behavior of the IEM which neglects the dependence of the ionization potential on the degree of ionization. The flat behavior of the curves for high values of P is related to the Magnus prediction of an ionization probability of 100% at small impact parameters. Accounting for the deviations between experiment and theory, there will be *55% L-shell ionization and complete valence-band ionization* inside a track diameter of about 1.6 Å for U projectiles at 5 MeV/u. Thus, there is an enormous high degree of ionization directly after the interaction of the projectile with the target-electron system. The influence of this initial stage of the track evolution on the electron dynamics at much longer time scales is investigated in the next section.

4. Auger energy-shifts

In Fig. 3 the energy reduction of ion-induced Auger lines relative to the corresponding electron-induced spectra is displayed. For the 2s2pV line, we have used the high-energy edge at 75% of the peak height for the corresponding energy determination in order to exclude a possible influence of multiple 2p-ionization. It is noted that we have not performed a correction for the influence of δ-electron cascades on the 2pVV line position (this

awaits a more detailed understanding of the line shape). The peak shifts in Fig. 3 increase monotonically with the interaction strength P and reach about 2 eV at $P = 3.7$. Furthermore, the shifts are very similar for the different Auger lines. Macroscopic charging of the B-doped Si samples can be excluded for the observed effect, since no indication of a peak shift could be found for incident electrons at different beam currents. Materials modification can be excluded as well, since the electron reference-spectra, taken before and after the ion-measurement cycles, are identical to within an uncertainty of ± 0.15 eV.

Thus, we attribute the measured shift in Fig. 3 to the nuclear-track potential induced by the reduced electron density due to ionization in the center of the track. Auger electrons are decelerated when they leave such a charged region. From our previous measurements of this effect for polypropylene and mylar [7,8], we estimate that the initial track potential directly after the interaction with the projectile will exceed 100 V for Xe^{31+} ions. Thus, the measured shift of only 2 eV is strongly influenced by the time dependent electronic neutralization of the track. For an exponential decay, however, a time dependence of the potential should show up in the three Auger line-shifts that cover effective decay times from about 1 to 50 fs. Hence, the major part of the neutralization is very rapid and the measured shift seems to be related to a very slow component that might be due to long-lived traps (excitons and defect states) in the amorphous material.

Fig. 4 displays normalized Si 2pVV Auger-electron structures for 5 MeV/u Ar^{16+} ions and projectile electrons at the same speed (taken in between the ion measurement cycles) on amorphous Si and Si(1 1 1) with 7×7 reconstruction. Subtraction of a continuous background and iterative separation of the contributions from multiple L-shell ionization has been performed with the data sets. It is emphasized that these spectra close to the Auger peak maximum are very insensitive to the details of the subtracted background [14]. Both spectra for crystalline Si have been reduced in energy by 0.82 eV. This structural shift is due to hydrogen-saturated bonds on top of the amorphous material which were removed from the crystalline sample at temperatures >1000 °C during the ion irradiation (experiments with improved target cooling do not show this effect).

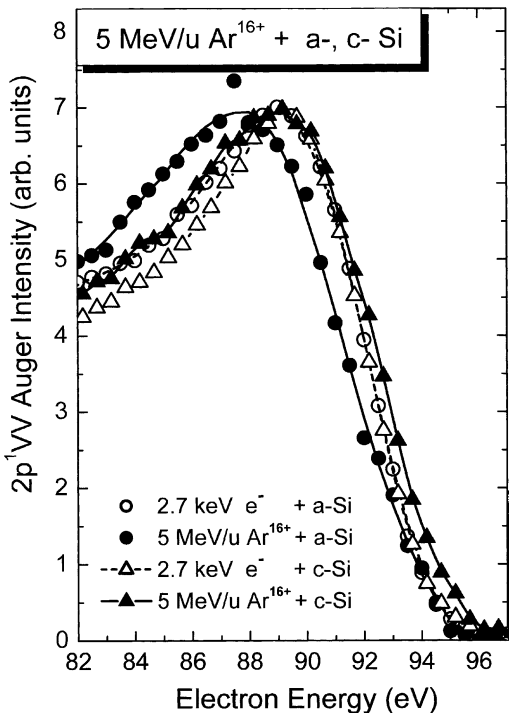

Fig. 4. 2pVV Auger-electron spectra for amorphous Si and crystalline Si(1 1 1) irradiated by electrons and Ar^{16+} ions.

From Fig. 4 it is seen that the spectral shapes as well as the line positions depend significantly on the type of projectile and on the phase of the target. The ion-induced lines show a broadening compared to the electron reference-data that might be related to high electron temperatures [10–12,14], but will not further be discussed here. The ion data for amorphous Si show an energy reduction of about 1.33 ± 0.20 eV as compared to the reference spectra (see also Fig. 3). The ion data for crystalline Si, however, show an energy reduction of only 0.35 ± 0.20 eV and the corresponding line shift for the $2p^2VV$ transition is even consistent with zero (-0.10 ± 0.25 eV). We take theses differences between the line shifts for the crystalline and amorphous Si samples as clear evidence for phase effects in the short-time dynamics of ion tracks in Si.

5. Conclusions

In this work we have presented Auger electron spectra induced by incident electrons and ions in the MeV/u regime. Spectra with excellent reproducibility have been taken for amorphous and single crystalline Si targets. The different investigated Auger lines and quantities correspond to snapshots of the track evolution for times between 10^{-18} s (vacancy production) and 5×10^{-14} s (Auger decay). The target surfaces, either amorphous Si or Si(1 1 1) with 7×7 reconstruction, were characterized by Auger-electron spectroscopy and LEED before and after the ion-irradiation runs. The analysis of multiple-ionization yields indicates in comparison with theory that there is *8–9-fold ionization* in the center of the ion tracks in Si, directly after the interaction with heavy projectiles ($Z > 14$). Hence, U projectiles at 5 MeV/u would produce an inner-shell ionization track of boron- or carbon-like target ions inside a track diameter of about 1.6 Å.

The $2p^n VV$- and 2s2pV-Auger electron structures show a shift towards lower energy when the charge of the projectile is increased. This finding points to a slow and weak component of the *nuclear-track potential* at the center of the ion track. Comparison of the Auger electron spectra for amorphous and crystalline Si gives, for the first time, evidence for *phase effects in the short-time dynamics* of ion tracks. Charge neutralization seems to be significantly slower in amorphous than in crystalline Si targets, leading to decelerated Auger electrons. A refined analysis, however, is necessary to separate effects due to the hot electronic system, showing up as increased line widths, and to derive improved quantitative results for the track potential.

Acknowledgements

We also acknowledge the support by the Alexander-von-Humboldt foundation and by the PROBRAL contract between DAAD and Capes.

References

[1] R.L. Fleischer, P.B. Price, R.M. Walker, Nuclear Tracks in Solids, University of California Press, Berkely California, 1975.
[2] R. Spohr, Ion Tracks and Microtechnology, F.Vieweg und Sohn Verlagsgesellschaft, Braunschweig, 1990.
[3] P. Stampfli, K.H. Bennemann, Phys. Rev. B 49 (1994) 7299;
P. Stampfli, Nucl. Instr. and Meth. B 107 (1996) 138.
[4] Z.G. Wang, C. Dufour, E. Paumier, M. Toulemonde, J. Phys.: Condens. Matter 6 (1994) 6733.
[5] A.E. Volkov, V.A. Borodin, Nucl. Instr. and Meth. B 107 (1996) 172.
[6] S. Klaumünzer, M.-D. Hou, G. Schumacher, Phys. Rev. Lett. 57 (1986) 850.
[7] G. Schiwietz, P.L. Grande, B. Skogvall, J.P. Biersack, R. Köhrbrück, K. Sommer, A. Schmoldt, P. Goppelt, I. Kádár, S. Ricz, U. Stettner, Phys. Rev. Lett. 69 (1992) 628.
[8] G. Schiwietz, G. Xiao, Nucl. Instr. and Meth. B 107 (1996) 113.
[9] G. Xiao, G. Schiwietz, P.L. Grande, A. Schmoldt, N. Stolterfoht, M. Grether, R. Köhrbrück, A. Spieler, U. Stettner, Phys. Rev. Lett. 79 (1997) 1821.
[10] G. Schiwietz, E. Luderer, G. Xiao, P.L. Grande, Nucl. Instr. and Meth. B 175–177 (2001) 1.
[11] G. Schiwietz, G. Xiao, P.L. Grande, E. Luderer, R. Pazirandeh, U. Stettner, Nucl. Instr. and Meth. B 146 (1998) 131;
Europhys. Lett. 47 (1999) 384;
G. Schiwietz, G. Xiao, E. Luderer, P.L. Grande, Nucl. Instr. and Meth. B 164 (2000) 353.
[12] M. Caron, H. Rothard, M. Beuve, B. Gervais, Phys. Scr. T 92 (2001) 281.
[13] K. Wien, Ch. Koch, Nguyen van Tan, Nucl. Instr. and Meth. B 100 (1995) 322.
[14] G. Schiwietz, E. Luderer, K. Czerski, M. Roth, F. Staufenbiel, P.L. Grande, Nucl. Instr. and Meth. B 193 (2002) 705, the assignment of a 2pVV surface-plasmon peak is false according to the present more detailed analysis.
[15] G. Schiwietz, D. Schneider, J.P. Biersack, N. Stolterfoht, D. Fink, A. Mattis, B. Skogvall, H. Altevogt, V. Montemayor, U. Stettner, Phys. Rev. Lett. 61 (1988) 2677.
[16] W. Schmidt, P. Müller, V. Brückner, F. Löffler, G. Saemann-Ischenko, W. Schubert, Phys. Rev. A 24 (1981) 2420.
[17] A. Koyama, H. Ishikawa, K. Maeda, Y. Sasa, O. Benka, M. Uda, Nucl. Instr. and Meth. B 48 (1990) 608.
[18] G. Schiwietz, P.L. Grande, Radiation Effects and Defects in Solids 130–131 (1994) 137 and references therein.
[19] M. Krause, J. Phys. Chem. Ref. Data 8 (1979) 507.
[20] M. Rösler, W. Brauer, Particle Induced Electron Emission I, Springer tracts of modern physics, Vol. 122, Springer, Berlin, 1991.